10-2013

Phase Diagram and Magnetocaloric Effects in Aluminum Doped MnNiGe Alloys

Abdiel Quetz
Southern Illinois University Carbondale

Tampas Samanta
Southern Illinois University Carbondale

Igor Dubenko
Southern Illinois University Carbondale

Michael J. Kangas

Julia Y. Chan

See next page for additional authors

Published in *Journal of Applied Physics* Vol. 114 No. 153909 (2013) at doi: 10.1063/1.4826260

Phase diagram and magnetocaloric effects in aluminum doped MnNiGe alloys

Abdiel Quetz,[1] Tapas Samanta,[1] Igor Dubenko,[1] Michael J. Kangas,[2] Julia Y. Chan,[3] Shane Stadler,[4] and Naushad Ali[1]
[1]*Department of Physics, Southern Illinois University, Carbondale, Illinois 62902, USA*
[2]*Department of Chemistry, Louisiana State University, Baton Rouge, Louisiana 70803, USA*
[3]*Department of Chemistry, University of Texas at Dallas, Richardson, Texas 75080, USA*
[4]*Department of Physics & Astronomy, Louisiana State University, Baton Rouge, Louisiana 70803, USA*

(Received 5 July 2013; accepted 4 October 2013; published online 21 October 2013)

The magnetocaloric and thermomagnetic properties of the $MnNiGe_{1-x}Al_x$ system have been studied by temperature-dependent x-ray diffraction, differential scanning calorimetry (DSC), and magnetization measurements. The partial substitution of Al for Ge in $MnNiGe_{1-x}Al_x$ results in a first order magnetostructural transition (MST) from a hexagonal ferromagnetic to an orthorhombic antiferromagnetic phase at 186 K (for $x = 0.09$). A large magnetic entropy change of $\Delta S_M = -17.6$ J/kg K for $\Delta H = 5$ T was observed in the vicinity of $T_M = 186$ K for $x = 0.09$. The value is comparable to those of giant magnetocaloric materials such as $Gd_5Si_2Ge_2$, $MnFeP_{0.45}As_{0.55}$, and $Ni_{50}Mn_{37}Sn_{13}$. The values of the latent heat ($L = 6.6$ J/g) and corresponding total entropy changes ($\Delta S_T = 35$ J/kg K) have been evaluated for the MST using DSC measurements. Large negative values of ΔS_M of -5.8 and -4.8 J/kg K for $\Delta H = 5$ T in the vicinity of T_C were observed for $x = 0.09$ and 0.085, respectively. A concentration-dependent phase diagram of transition temperatures (magnetic, structural, and magnetostructural) has been generated using magnetic, XRD, and DSC data. The role of magnetic and structural changes on transition temperatures is discussed. © *2013 AIP Publishing LLC*. [http://dx.doi.org/10.1063/1.4826260]

I. INTRODUCTION

MnNiGe based intermetallic compounds belong to the family of the magnetic materials that undergo magnetostructural transitions (MST) near room temperature.[1] Such transitions are of great interest from fundamental and technological points of view due to their significant magnetoresponsive behaviors, resulting in unique phenomena such as giant magnetocaloric effects,[1–3] magnetoresistance,[4] magnetostriction,[5] and magnetic shape memory, etc.

Stoichiometric MnNiGe undergoes a first order structural transition (FOT) from a low-temperature phase (LTP), i.e., an orthorhombic TiNiSi-type crystal structure, to a high-temperature hexagonal Ni_2In-type structure at 470 K. Both phases are in paramagnetic states in the vicinity and above the FOT. The low temperature phase is magnetically ordered below $T_N \sim 346$ K with a spiral antiferromagnetic (AFM) structure.[6] Recently, it has been found that changes in stoichiometry and chemical composition can drastically change the FOT temperature. In some cases the structural transformation occurs below T_N of the LTP and therefore results in a first order change of magnetic state of the MnNiGe based compounds.[7–10] The Mn-Mn distance has been considered as a major factor affecting the crystal phase stability in these compounds.[7,8,11] However, most studies have considered systems with constricted lattices with respect to the parent compounds.[7,8,11] In a previous study (see Ref. 12), we show that the expansion of the lattice cell, as observed for $MnNiGe_{1-x}Al_x$, results in the formation of an MST from a hexagonal ferromagnetic to an orthorhombic antiferromagnetic phase at 193 K and 186 K for $x = 0.085$ and 0.09, respectively. The values of the latent heat (L), corresponding to total entropy changes (ΔS_T) and magnetic-field-induced entropy changes (ΔS_M) in the vicinity of the MST, were found to be $L = 6.6$ J/g, $\Delta S_T = 35$ J/kg K, and $\Delta S_M = 17.6$ J/kg K (for $\Delta H = 5$ T), respectively. The magnetocaloric effect (MCE) parameters observed for the $MnNiGe_{1-x}Al_x$ system are comparable to well-known giant magnetocaloric materials such as $Gd_5Si_2Ge_2$,[16] $Ni_{50}Mn_{37}Sn_{13}$,[3] and $MnFeP_{0.45}As_{0.55}$.[2] Therefore, a detailed knowledge of the influence of Al substitution on phase transitions and magnetocaloric effects of MnNiGe are desirable. In the current work, results of the studies of the fractional substitution of Ge by Al on the magnetic, magnetocaloric, and structural properties of the $MnNiGe_{1-x}Al_x$ compound with $0 < x < 0.20$ along with the magnetic phase diagram are reported.

II. EXPERIMENTAL TECHNIQUES

The $MnNiGe_{1-x}Al_x$ aluminum doped samples with $0 < x < 0.20$ were arc-melted in an ultra-high purity argon atmosphere using 99.99% purity elements. The compounds were annealed in high vacuum ($\approx 10^{-5}$ Torr) for 96 h at a temperature of 850 °C. XRD with Cu $K\alpha$ radiation was implemented to measure the room temperature diffraction patterns, and the Rietveld profile refinement method was employed within the FULLPROF program to obtain the structural properties of the samples. The X-ray diffraction measurements in the temperature interval (100–370 K) have been done using a single crystal with size $\sim 0.1 \times 0.1 \times 0.1$ mm that was selected from a crushed polycrystalline ingot of $NiMnGe_{0.91}Al_{0.09}$ (nominal composition). The crystal was then mounted on a glass fiber with epoxy, coated in vacuum

grease, and placed on the goniometer of a Nonius Kappa CCD X-ray diffractometer with a Mo Kα radiation ($\lambda = 0.71073$ Å) source. All temperature ramp rates were 60 K/h to minimize stress on the crystal. For crystal structure determinations, the crystal was held at the target temperature for a minimum of 20 min to ensure the crystal was equilibrated. XRD data were collected at 370, 296, 200, and 100 K. The crystal structure was solved by direct methods with SIR97[19] and refined with SHELXL97.[20] Lattice parameters as a function of temperature were collected by first warming the crystal to 370 K and cooling to 100 K. The magnetization measurements were obtained in a temperature interval of 5 to 380 K at magnetic fields up to 5 T using a superconducting quantum interference device magnetometer (SQUID by Quantum Design). The differential scanning calorimetry (DSC) measurements were obtained using a DSC 8000 instrument (with a ramp rate of 20 K/min during heating and cooling) in the temperature range of 103–573 K. The latent heat (L) was estimated from the endothermic peak of the heat flow curve using $L = \int_{T_s}^{T_f} \frac{dQ}{dT} dT$, where $\frac{dQ}{dT}$ is the change of heat flow with respect to temperature, and T_s and T_f are the initial and final temperatures of the magnetostructural phase transitions on heating, respectively.

III. RESULTS AND DISCUSSION

The orthorhombic TiNiSi-type and hexagonal Ni_2In-type crystal structures were identified from XRD patterns of the $MnNiGe_{1-x}Al_x$ samples at room temperature for the compounds with $x \leq 0.03$ and $x \geq 0.5$, respectively (see Figure 1 for representative compounds). As can be seen from Figure 2, the M(H) curves are characterized by different behaviors depending on Al concentration. At least two types of M(H) curves were detected. The compounds with $x \leq 0.095$ demonstrate a behavior typical for antiferromagnetic ordering with compensated magnetization at zero-field and a "spin-flip"-like transition (SFT) induced by magnetic field. The parent compounds have spiraled AFM structures;

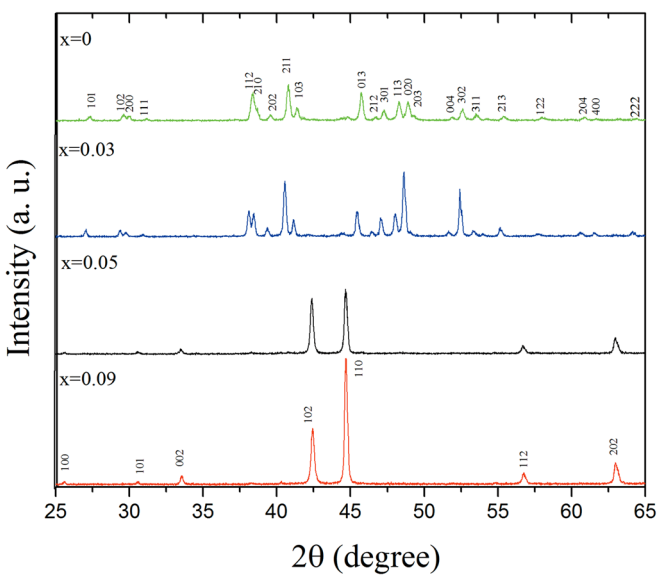

FIG. 1. The XRD patterns of $MnNiGe_{1-x}Al_x$ for different aluminum concentrations (x) at room temperature.

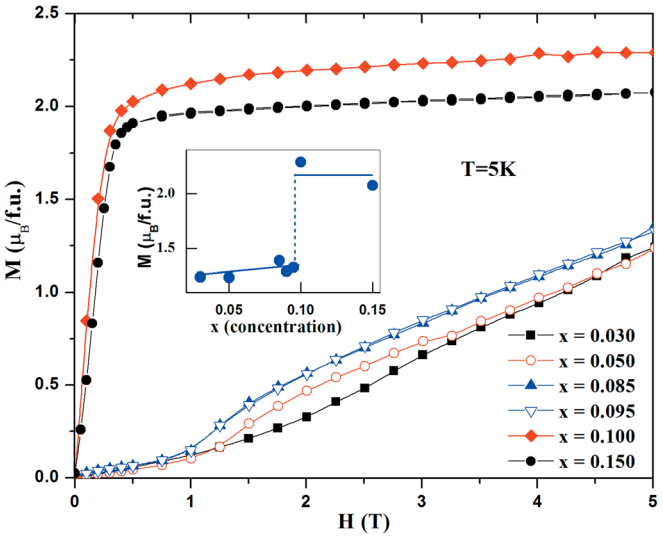

FIG. 2. The M(H) of $MnNiGe_{1-x}Al_x$ for $0.03 < x < 0.150$ at T = 5 K. Inset: The magnetic moment of $MnNiGe_{1-x}Al_x$ system at 5 T.

therefore, the observed transitions can be associated with a transition from a spiral AFM to a non-collinear state induced by magnetic field. Increasing the Al concentration results in a decrease in the critical field of the SFT to 1.2 T for x = 0.05, which most likely results from a decrease of the magnetocrystalline anisotropy.

The compounds with $x \geq 0.1$ show ferromagnetic-like magnetization curves with a magnetic moment ~2.0 μ_B/f.u. at 5 T, an anisotropy field $H_A \sim 1.5$ T, and a magnetic susceptibility $\chi_o \sim 0.2\ \mu_B$/f.u./T at $H > H_A$. The relatively large χ_o detected for the compounds in the ferromagnetic state is evidence of itinerant characteristics of the magnetism. The increase in the magnetization at 5 T by a factor of 2 indicates a change in the magnetic ordering induced by the Al (see inset of Figure 2). Thus, the magnetic ground state depends on Al concentration and changes from AFM to FM ordering at the critical aluminum concentration $x_C \approx 0.1$.

The temperature dependence of the magnetization measured in applied fields of 0.1 T and 5 T is shown in Figure 3.

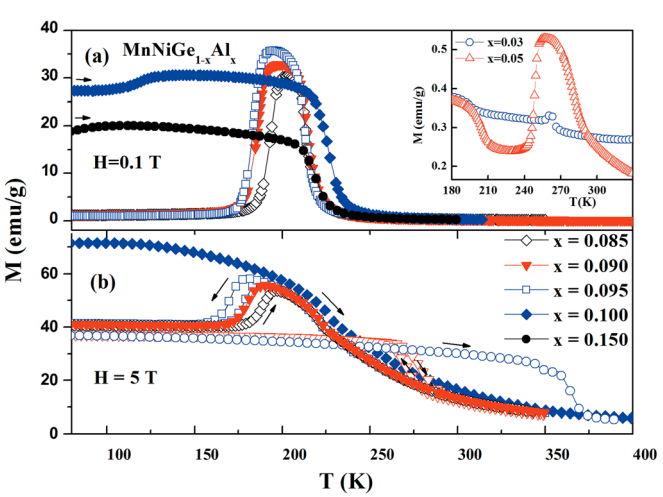

FIG. 3. (a) The M(T) curves for $MnNiGe_{1-x}Al_x$ obtained for heating cycles at H = 0.1 T. Inset: M(T) for x = 0.03 and x = 0.05, and (b) The M(T) curves obtained at H = 5 T for heating and cooling as indicated by the arrows.

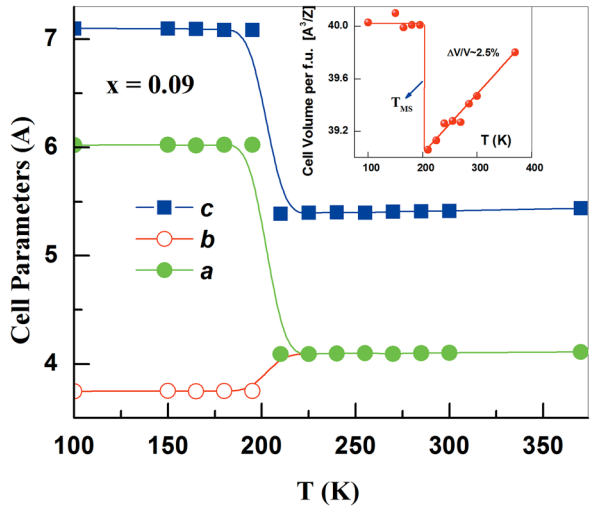

FIG. 4. Temperature dependence of the cell parameters of $MnNiGe_{0.91}Al_{0.09}$. Inset: $MnNiGe_{0.91}Al_{0.09}$ cell volume with respect to temperature.

The $MnNiGe_{1-x}Al_x$ system exhibits three distinct temperature dependent behavior regimes, depending on Al concentration. The Ge–rich samples ($x \leq 0.05$) exhibit a maximum in the M(T) curves at the $T = T_N$ (see inset of Figure 3(a)) and a temperature hysteresis of M(T) (see Figure 3(b)). Taking into account the AFM-type of magnetization at 5 K (see Figure 2), and the similar temperature-dependent behavior of the magnetization of the parent MnNiGe,[6] it is natural to relate the transitions observed for compounds with $x \leq 0.05$ to a structural martensitic-like transition from a hexagonal AF to an orthorhombic AF structure.

The compounds with $x \geq 0.1$ show M(T) curves consistent with ferromagnetic behavior. At least two phase transitions are clearly seen in the M(T) curves of $MnNiGe_{1-x}Al_x$ with $0.05 < x < 0.1$. These are the low temperature transitions with jump-like increases in magnetization at $T = T_{MS}$ with thermal hysteresis, and a high temperature transition to a paramagnetic state at T_C. Considering the magnetization curves M(H) in the vicinity of the phase transitions, one can conclude that the low and high-temperature transitions are from AF to FM and from FM to PM, respectively.

The temperature-dependent XRD study of the crystal structure of $MnNiGe_{0.91}Al_{0.09}$ has been carried out to clarify the nature of the low temperature transitions. As observed in Figure 4, a jump-like change in the cell parameters, as well as an increase in cell volume (see inset of Figure 4), takes place in the vicinity of $T_M \sim 200$ K. At room temperature, the diffraction pattern was indexed to a hexagonal unit cell (see Table I). Systematic peak absences indicated the space group

TABLE I. Cell parameters of $MnNiGe_{1-x}Al_x$ system at room temperature.

x	c (Å)	a (Å)	c/a	Volume $(Å)^3$
0.05	5.429	4.098	1.325	78.99
0.07	5.428	4.099	1.324	79.00
0.085	5.425	4.100	1.323	79.00
0.09	5.426	4.102	1.323	78.92
0.1	5.425	4.108	1.321	79.30
0.15	5.425	4.102	1.322	79.06

TABLE II. Crystallographic parameters of $NiMnGe_{0.91}Al_{0.09}$ for 100 K (orthorhombic), and 296 K (hexagonal).

Compound	$NiMnGe_{0.91}Al_{0.09}$	$NiMnGe_{0.91}Al_{0.09}$
Crystal system	Hexagonal	Orthorhombic
Space group	$P6_3/mmc$	$Pnma$
a (Å)	4.102(2)	6.015 (1)
b (Å)	4.102(2)	3.734(2)
c (Å)	5.416(3)	7.089(2)
V $(Å)^3$	78.92(7)	159.22(10)
Z	2	4
Refinement		
R_1	0.0275	0.0227
wR_2	0.0721	0.0548

to be $P6_3/mmc$. In the refinement procedures, the aluminum was initially placed on the germanium site (based on stoichiometry) and the occupancy was refined. Because the refined occupancy of aluminum (8%) was close to the nominal composition (9%), the aluminum was kept on the germanium site and fixed to the nominal value. The structures at 200 K and 370 K were consistent with the room temperature polymorph. At 100 K, the crystal structure of $NiMnGe_{0.91}Al_{0.09}$ was found to adopt the previously reported[6] low temperature polymorph of NiMnGe (*Pnma*). Details of the collection/refinement and atomic positions are provided in Table II for 100 K and 296 K. Therefore, as confirmed by these temperature-dependent XRD results, the first order, low temperature transitions observed for $MnNiGe_{1-x}Al_x$ with $0.05 < x < 0.1$ are magnetostructural transitions. It is also interesting to note that the transitions are accompanied by a giant positive volume anomaly $\Delta V/V$ of about 2.5% (see inset of Figure 4). The first order nature of the phase transitions observed in $MnNiGe_{1-x}Al_x$ $x < 0.1$ has been also confirmed by the temperature hysteresis of heat flow transition peaks obtained from DSC measurements (see Figure 5). The large endothermic/exothermic peaks, observed during heating/cooling cycles, were also observed in previous experiments for MST samples in this system,[12] and are related

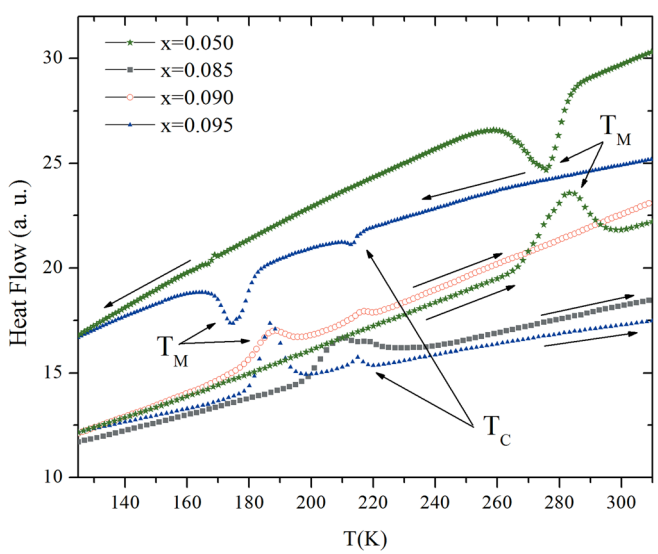

FIG. 5. DSC heat flow curves as a function of temperature for MnNi(Ge,Al) obtained for cooling and heating cycles as indicated by the arrows.

to the latent heat of the first-order magnetostructural transition from the antiferromagnetic TiNiSi-type structure to the ferromagnetic Ni_2In-type structure. The temperature hysteresis of heat flow of about 20 K between heating and cooling cycles detected from DSC measurements are consistent with magnetization results.

The variations of the phase transition temperatures as a function of Al concentration are summarized in the (T-x)-phase diagram (see Figure 6). An increase in Al content results in an increase of the phase transition temperatures related to the changes in magnetic ordering at T_N and T_C in the orthorhombic ($0 \le x \le 0.03$) and hexagonal phases ($0.08 \le x \le 0.15$), respectively. The temperatures of the structural transitions T_M and T_{MS} decrease with increasing Al concentration, and abruptly vanish at some critical Al concentration in the interval $0.095 < x \le 0.10$; as a consequence only the hexagonal phase is present for $x \ge 0.1$.

The concentration of conduction electrons per atom (e/A) and dimensional factors (such as crystal cell parameters, volume, degree of the tetragonal distortions, and c/a), are traceable, experimental factors affecting the phase transitions in magnetic Heusler alloys.[13] Since Al has fewer valence electrons and a larger metallic radius compared to Ge, the substitution of Ge with Al in $MnNiGe_{1-x}Al_x$ up to $x = 0.15$ results in a decrease of about 0.4% in electronic concentration and an increase of ~0.1% in cell volume (see Table I). The behavior of the structural transition temperatures is consistent with the results reported in Ref. 14 where a decrease in T_M of about 210 K was observed for a ~0.1% change in e/a.

As shown in the inset of the Figure 6, Al substitution induces a decrease in the c lattice parameter, and a decrease in the degree of hexagonal distortion (c/a-ratio). It has been found from band structure calculations that the free energy of the martensitic phase depends on the c/a ratio.[15] Thus, based on these results and observed behaviors, it can be concluded that the increase of cell volume of the austenitic phase results in a loss of martensitic phase stability, similar to that observed in the case of the $Ni_2Mn(Ga,In)$ system in Ref. 16. Therefore, there is the range of c/a values where the martensitic transformation can be observed. In the case of the $MnNiGe_{1-x}Al_x$ compounds, when $c/a > 1.323$ the high temperature hexagonal phase is stable for all temperatures.

Two factors affecting the magnetic ordering temperatures T_N and T_C for $0 \le x \le 0.03$ and $0.085 < x \le 0.15$, respectively, can be highlighted based on the results. These are related to the changes in the electron concentration (e/a) and Mn-Mn distance as a result of Al substitution. If the $N(E_F)$ has a positive curvature in the vicinity of E_F, a decrease in e/a results in an increase in $N(E_F)$, and therefore in the net magnetic moment of itinerant electrons (or in the magnetic moment of the magnetic sublattice in the case of AF ordering) and subsequently in the free energy terms related to exchange interactions, similar to that observed in the case of $Y(Co,Al)_2$ compounds.[17] As a result, both T_N and T_C increase with Al-concentration in $MnNiGe_{1-x}Al_x$. The Mn-Mn distance increases and decreases in-plane and along the c axis, respectively (see inset of Figure 6). Such changes can affect the delicate balance of the positive and negative exchange interactions that account for the antiferromagnetic, spiral-like magnetic structure of the parent compound, and results in an increase of the ordering temperatures of the compounds under consideration. However, taking into account that the T_N and T_C lines in the phase diagram (see the blue dot-dashed lines in Fig. 6) are nearly parallel, the first mechanism is preferable. Thus, Al substitution tends to increase the magnetic moment by shifting E_F toward the maximum of $N(E_F)$, and results in an increase of T_N and T_C, putting the system into a high magnetization state for $x > 0.90$.

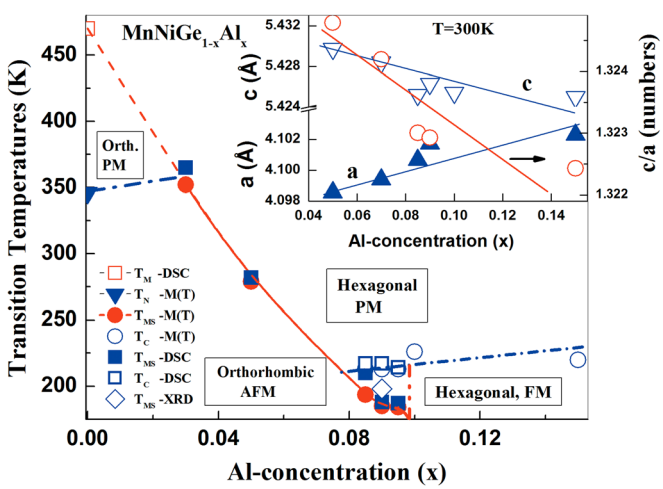

FIG. 6. Temperature of the magnetic (T_N, T_C), structural (T_M), and magnetostructural (T_{MS}) transitions with respect to Al concentration (x) obtained from different types of measurements as labeled. Inset: The concentration dependence of the cell parameters a and c and the c/a ratio obtained at T = 300 K for hexagonal MnNi(Ge,Al) compounds.

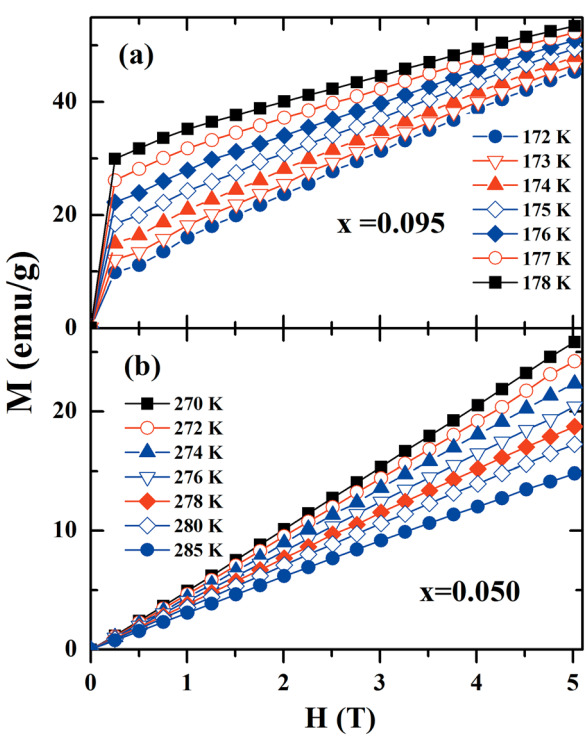

FIG. 7. Isothermal M(H) curves in the vicinity of the magnetostructural phase transitions.

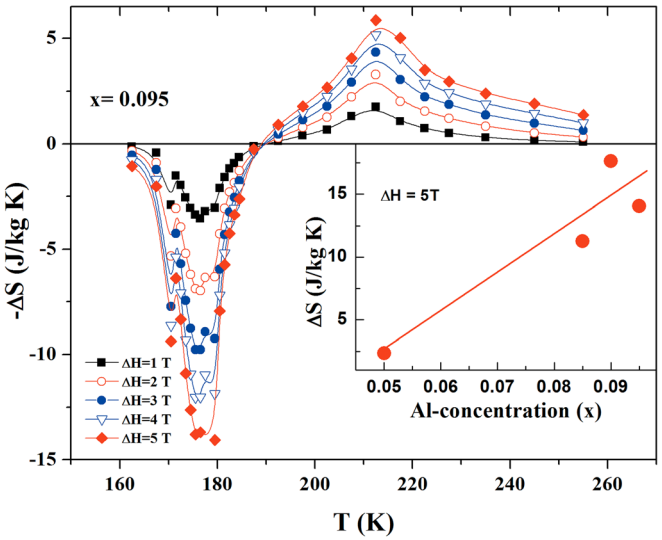

FIG. 8. The characteristic entropy changes in the vicinity of the magnetostructural transition at different applied fields, as shown for $MnNi(Ge_{0.905}Al_{0.095})$. Inset: The entropy changes obtained for $\Delta H = 5$ T with respect to Al concentration (x).

The change in the magnetic behavior in the vicinity of magnetostrucstural transitions from orthorhombic antiferromagnetic to hexagonal ferromagnetic and from orthorhombic antiferromagnetic to hexagonal paramagnetic phases are shown in Figures 7(a) and 7(b), respectively. As shown in Fig. 7(a), the magnetization curves show a gradual transition to ferromagnetism starting at 172–178 K and are associated with a field-induced reverse martensitic transformation. The magnetic entropy changes (ΔS_M) were calculated using the Maxwell relation, $(\partial S/\partial H)_T = (\partial M/\partial T)_H$, from the magnetization isotherms measured at different temperatures.[18] The $\Delta S_M(T)$ curves for different changes in magnetic field (ΔH) are shown in Figure 8. A large inverse MCE has been observed in the vicinity of T_M, which is associated with the rapid change of magnetization (see Figure 3) due to the AF-FM first-order magnetostructural transition.

IV. CONCLUSION

We have studied the influence of the partial substitution of Ge by Al on the magnetostructural and magnetocaloric properties of MnNiGe. An Al-concentration-dependent phase diagram has been constructed to elucidate the magnetic/magnetostructural properties of the materials and to summarize the different types of magnetic/magnetostructural transitions observed in this system. For small Al concentrations ($x \leq 0.03$), the system exhibits a PM-AFM, second order transition in a low-temperature orthorhombic phase with decreasing temperature. However, the substitution of higher Al concentrations results in a SOT from a FM to a PM state in its high-temperature hexagonal phase before showing a MST from an AFM to a FM state in the intermediate composition range ($0.085 \leq x \leq 0.095$). The MST from an AFM to a FM state results in a large inverse MCE in the vicinity of T_M for compounds with $x = 0.085$, 0.090, and 0.095. In general, the $MnNiGe_{1-x}Al_x$ compounds undergo remarkable changes in their magnetic properties and exhibit magnetostructural transitions which make them of interest due to their potential application in magnetic refrigeration.

ACKNOWLEDGMENTS

This work was supported by the Office of Basic Energy Sciences, Material Science Division of the U.S. Department of Energy (DOE Grant Nos. DE-FG02-06ER46291 and DE-FG02-13ER46946). J.Y.C. acknowledges support from the National Science Foundation (NSF-DMR 1063735).

[1]A. O. Pecharsky, K. A. Gschneidner, Jr., and V. K. Pecharsky, J. Appl. Phys. **93**, 4722 (2003).
[2]O. Tegus, E. Bruck, K. H. J. Buschow, and F. R. de Boer, Nature (London) **415**, 150 (2002).
[3]T. Krenke, E. Duman, M. Acet, E. F. Wassermann, X. Moya, L. Mañosa, and A. Planes, Nat. Mater. **4**, 450 (2005).
[4]S. Y. Yu, Z. H. Liu, G. D. Liu, J. L. Chen, Z. X. Cao, G. H. Wu, B. Zhang, and X. X. Zhang, Appl. Phys. Lett. **89**, 162503 (2006).
[5]R. Kainuma, Y. Imano, W. Ito, Y. Sutou, H. Morito, S. Okamoto, O. Kitakami, K. Oikawa, A. Fujita, T. Kanomata, and K. Ishida, Nature (London) **439**, 957 (2006).
[6]W. Bazela, A. Szytuła, T. Todorović, Z. Tomkowicz, and A. Zieba, Phys. Status Solidi A **38**, 721 (1976).
[7]C. L. Zhang, D. H. Wang, Q. Q. Cao, Z. D. Han, H. C. Xuan, and Y. W. Du, Appl. Phys. Lett. **93**, 122505 (2008).
[8]C. Zhang, D. Wang, Q. Cao, S. Ma, H. Xuan, and Y. Du, J. Phys. D: Appl. Phys. **43**, 205003 (2010).
[9]Z. C. Liang, W. D. Hui, C. Jian, W. T. Zhi, X. G. Xi, and Z. Chun, Chin. Phys. B **20**, 097501 (2011).
[10]E. Liu, Y. Du, J. Chen, W. Wang, H. Zhang, and G. Wu, IEEE Trans. Magn. **47**, 4041 (2011).
[11]J. T. Wang, D. S. Wang, C. F. Chen, O. Nashima, T. Kanomata, H. Mizuseki, and Y. Kawazoe, Appl. Phys. Lett. **89**, 262504 (2006).
[12]T. Samanta, I. Dubenko, A. Quetz, S. Temple, S. Standler, and N. Ali, Appl. Phys. Lett. **100**, 052404 (2012).
[13]P. Entel, V. D. Buchelnikov, V. V. Khovailo, A. T. Zayak, W. A. Adeagbo, M. E. Gruner, H. C. Herper, and E. F. Wassermann, "Modelling the phase diagram of magnetic shape memory Heusler alloys," J. Phys. D: Appl. Phys. **39**, 865–889 (2006).
[14]E. K. Liu, W. Zhu, L. Feng, J. L. Chen, W. H. Wang, G. H. Wu1, H. Y. Liu, F. B. Meng, H. Z. Luo, and Y. X. Li, "Vacancy-tuned paramagnetic/ferromagnetic martensitic transformation in Mn-poor $Mn_{1-x}CoGe$ alloys," EPL **91**, 17003 (2010).
[15]A. Ayuela, J. Enkovaara, K. Ullako, and R. M. Neiminen, J. Phys. Condens. Matter **11**, 2017 (1999).
[16]M. Khan, I. Dubenko, S. Stadler, and N. Ali, "Magnetic and structural phase transitions in Heusler type alloys $Ni_2MnGa_{1-x}In_x$," J. Phys.: Condens. Matter **16**, 5259–5266 (2004).
[17]R. Z. Levitin and A. S. Markosyan, "Itinerant Metamagnetism," Usp. Fiz. Nauk **155**, 623–657 (1988); I. L. Gabelko, R. Z. Levitin, A. S. Markosyan, V. I. Silantiev, and V. V. Snegirev, "Itinerant metamagnetism and ferromagnetism in the M(Col -,Al,), (M EY and Lu) systems: The effect of unit cell volume," Zh. Eksp. Teor. Fiz. **98**, 2067–2073 (1990).
[18]K. A. Gschneidner, Jr., V. K. Pecharsky, and A. O. Tsokol, Rep. Prog. Phys. **68**, 1479 (2005).
[19]A. Altomare, M. C. Burla, M. Camalli, G. L. Cascarano, C. Giacovazzo, A. Guagliardi, A. G. G. Moliterni, G. Polidori, and R. Spagna, "SIR97: A new tool for crystal structure determination and refinement," J. Appl. Crystallogr. **32**, 115–119 (1999).
[20]G. Sheldrick, "A short history of SHELX," Acta Crystallogr. A **64**, 112–122 (2008).